ROYAL SOCIETY
OF CHEMISTRY

PAPER

Check for updates

Direct synthesis of fluorinated hyperbranched polyethylenes by chain walking copolymerization†

Peishuai Dai,[a] Naiheng Song[b] and Zhibin Ye [ID] *[a]

Hyperbranched polyethylenes synthesized *via* Pd–diimine chain walking polymerization possess distinctive structural features. Incorporation of fluorine is anticipated to further enhance their performance by imparting valuable attributes and thereby expanding their potential applications. In this work, we present the synthesis of a new series of fluorinated hyperbranched polyethylenes through chain walking copolymerization of ethylene with various fluorinated comonomers. The comonomers investigated herein include hexafluoroisopropyl acrylate (HFIPA), allylpentafluorobenzene (APFB), tridecafluorooctyl(allyl) ether (13FOAE), and 1*H*,1*H*,2*H*-perfluoro-1-hexene (PFH), with APFB, 13FOAE, and PFH employed for the first time in this polymerization system. The choice of comonomers markedly influences catalyst activity and incorporation efficiency. Three comonomers, *i.e.*, HFIPA, APFB, and 13FOAE, were found to be copolymerizable under the reaction conditions, with APFB delivering the highest catalytic activity and 13FOAE achieving the highest comonomer incorporation at identical feed concentrations. Notably, even a low-level incorporation of fluorinated comonomers substantially reduces the surface energy of the resulting copolymers, while retaining their hyperbranched topology and low glass-transition temperature (*ca.* −69 °C).

Introduction

Despite their potential environmental implications, fluorinated polymers have attracted significant attention due to their unique physical and chemical properties, which make them essential for highly specialized applications. The carbon–fluorine bond has a high bond dissociation energy of 480 kJ mol^{-1}, significantly greater than that of the carbon–hydrogen bond (around 410 kJ mol^{-1}).[1] This high bond energy leads to low polarizability and exceptional bond stability, imparting fluoropolymers with outstanding properties such as low solubility, low friction, high dielectric strength, and excellent thermal and chemical stability.[2] Consequently, fluoropolymers have been extensively applied in high-performance coatings, fuel cell membranes, optical materials, and aerospace applications.

Integrating the desirable features of fluoropolymers into novel polymer architectures offers an attractive pathway to develop advanced materials with tailored properties. Hyperbranched polyethylene (HBPE) is a distinctive class of polyethylene featuring a highly branched three-dimensional architecture resembling that of dendrimers. HBPE demon-

strates advantageous characteristics, such as low solution and melt viscosity, and enhanced solubility,[3,4] and has been employed in diverse applications including lubricant viscosity modifiers,[5] polymer processing aids (PPA),[6] and functional polymers for the dispersion and solubilization of carbon nanotubes in organic solvents.[7] However, due to its inherently nonpolar nature and lack of specific functional groups, the application of HBPE as a multifunctional material remains limited. To address these limitations and broaden its applicability, introducing polar functionalities into the polymer structure has become a key strategy. Among various modifications, fluorinated HBPE is expected to have a unique combination of HBPE's architecture with exceptional properties of fluoropolymers. Incorporating fluorinated groups into the HBPE structure can impart enhanced hydrophobicity, superior chemical and thermal resistance, and tunable surface/interfacial properties. These attributes are particularly advantageous for high-performance applications in demanding environments requiring robust chemical stability and engineered surface functionality.

Industrial strategies for synthesizing functionalized polyethylene typically rely on free-radical copolymerization of ethylene with polar comonomers. However, this approach typically requires harsh conditions (temperature above 150 °C and pressure exceeding 100 MPa).[8,9] In contrast, catalytic processes are highly desirable because they operate under much milder conditions. Unfortunately, early-transition metal catalysts with higher oxophilicity, commonly used in industrial processes,

[a]Department of Chemical and Materials Engineering, Concordia University, Montreal, Quebec H3G 1M8, Canada. E-mail: zhibin.ye@concordia.ca
[b]Aerospace Research Center, National Research Council of Canada, 1200 Montreal Road, Ottawa, Ontario K1A 0R6, Canada
†Dedicated to Professor Wenhua Sun on the occasion of his retirement.

are easily poisoned by polar monomers. While the copolymerization of ethylene with polar monomers has been achieved in a few special cases through protection of the polar functional groups, such strategies are often impractical for large-scale production.[10,11]

Recent advances in late-transition metal catalysts have offered new strategies for the efficient copolymerization of ethylene with polar monomers under milder conditions.[12] Representative systems include palladium–diimine catalysts developed by Brookhart *et al.* and neutral nickel catalysts by Grubbs *et al.*,[13] both demonstrating the capability to copolymerize ethylene with acrylates, polar norbornenes, and other functional comonomers. Among these, Pd–diimine catalysts are particularly noteworthy. Aside from the chain walking mechanism enabling the synthesis of the HBPE architecture, they also feature low oxophilicity and possess excellent tolerance toward various polar functional groups (*e.g.*, esters and halides), facilitating the synthesis of functionalized HBPEs by direct copolymerization of ethylene with polar monomers, such as functionalized acrylates and α-olefins.[12,14–16]

Pd–diimine catalysts have shown strong potential for the synthesis of fluorinated HBPEs. Previous studies have demonstrated that these catalysts can successfully copolymerize ethylene with semifluorinated acrylates containing fluorocarbons of various chain lengths to afford fluorinated HBPEs. However, the monomers explored to date have been limited to semifluorinated acrylates, which generally exhibit low reactivity during copolymerization. As a result, the resulting copolymers typically contain low fluorine contents.[17] To broaden the synthetic toolbox for more versatile synthesis of fluorinated HBPEs with enhanced fluorine contents, we investigate here the direct copolymerization of ethylene with a range of structurally distinct fluorinated monomers using a representative Pd–diimine catalyst. The fluorinated monomers investigated include allylpentafluorobenzene (APFB), tridecafluorooctyl (allyl) ether (13FOAE), and 1*H*,1*H*,2*H*-perfluoro-1-hexene (PFH), as well as hexafluoroisopropyl acrylate (HFIPA) as a benchmark fluorinated acrylate for comparison. These monomers vary in the spacer structure between the vinyl and the fluorinated groups, enabling the assessment of how the spacer

structure influences monomer reactivity. In addition, by systematically varying the comonomer feed concentrations, we examine the effects on catalyst activity and copolymer structures and property characteristics, including branching density, comonomer incorporation, molecular weight distribution, and thermal properties. This study not only expands the range of fluorinated monomers compatible with the Pd–diimine catalyst but also proposes a monomer design strategy for the catalytic synthesis of fluorinated polyethylenes (Scheme 1).

Experimental section

Materials

All manipulations involving oxygen- and moisture-sensitive compounds were carried out using standard Schlenk techniques or in an argon-filled glovebox. The Pd–diimine catalyst (Pd-1), [(ArN═C(Me)–(Me)C═NAr)Pd(CH$_3$)(N≡CMe)]SbF$_6$ (Ar = 2,6-(iPr)$_2$C$_6$H$_3$), was synthesized following a literature procedure.[16] Fluorinated monomers, including HFIPA (>98.0%), APFB (>98%), and PFH (>97%), were purchased from Aldrich and were dried over 3 Å molecular sieves prior to use. 13FOAE was synthesized according to a literature procedure.[18] Ultrahigh purity N$_2$ and polymer-grade ethylene (both from Air Liquide) were purified by passing through 3 Å/5 Å molecular sieves and Oxiclear columns to remove moisture and oxygen, respectively, before use. Allyl benzene (98%) and 4-phenyl-1-butene (99%) were obtained from Aldrich and were dried over 3 Å molecular sieves before use. Other chemicals, including deuterated chloroform (99.8 atom% D), anhydrous dichloromethane (CH$_2$Cl$_2$, ACS reagent), methanol (ACS reagent grade), tetrahydrofuran (THF, ACS reagent grade), diethyl ether (ACS reagent, anhydrous), concentrated hydrochloric acid (37%), hydrogen peroxide (H$_2$O$_2$, 50 wt% in water), tetrabutylammonium hydroxide (99%), allyl bromide (99%), 1*H*,1*H*,2*H*,2*H*-perfluoro-1-octanol (97%), and anhydrous sodium sulfate, were obtained from Aldrich and used as received. Deionized (DI) water was obtained using a Milli-Q purification system.
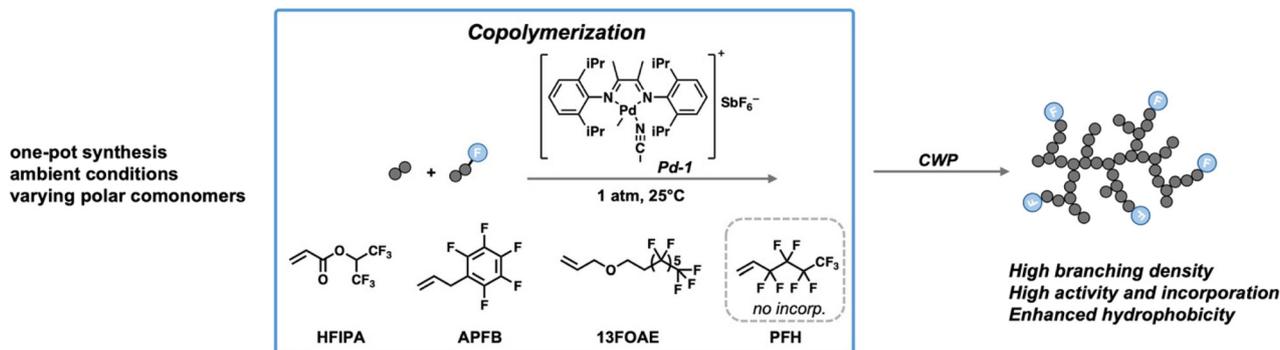
Scheme 1 Schematic synthesis of fluorinated HBPEs by Pd–diimine catalyzed ethylene copolymerization with different fluorinated comonomers.

Synthesis of tridecafluorooctylallyl ether (13FOAE)

$1H,1H,2H,2H$-Perfluoro-1-octanol (5 g, 13.7 mmol) was added into an aqueous solution of 20 M NaOH (2.42 g, 41.2 mmol). The mixture was stirred for 30 min at 50 °C, followed by the addition of diethyl ether (2.42 g, 32.7 mmol), and tetrabutylammonium hydroxide (0.09 g, 0.27 mmol) as the phase transfer agent. Allyl bromide (4.98 g, 41.2 mmol) was then added into the mixture. The reaction solution was stirred for 12 h at 50 °C under N_2. After the reaction was completed, diethyl ether was added to the mixture. The aqueous phase was removed, and the organic phase was washed three times with DI water (40 mL). The organic phase was dried with anhydrous sodium sulfate overnight and filtered. Subsequently, diethyl ether was removed under reduced pressure at 50 °C. The product (4.22 g, yield: 76%) was obtained as a colorless liquid. ^1H NMR (300 MHz, CDCl$_3$): δ (ppm) 5.90 (m, J = 17.2, 10.3, 5.6 Hz, 1H), 5.29 (dq, J = 17.2, 1.6 Hz, 1H), 5.21 (dq, J = 10.4, 1.4 Hz, 1H), 4.01 (dt, J = 5.6, 1.4 Hz, 2H), 3.73 (t, J = 6.9 Hz, 2H), 2.54–2.30 (m, 2H).

Polymerization procedure

All polymerizations were carried out in a 50 mL glass reactor equipped with a magnetic stirrer and a thermometer. In a typical run, the glass reactor was first dried overnight at 100 °C in an oven, followed by sealing with a rubber septum and cooling to room temperature under vacuum. The reactor was immersed in a constant-temperature oil bath set to the desired temperature. The reactor was purged with ethylene at least three times before being pressurized with ethylene to 1 atm. A specified amount of comonomer and the required volume of anhydrous CH_2Cl_2 were injected into the reactor. After thermal equilibration for 10 min, 0.1 mmol of Pd–diimine catalyst in 2 mL of anhydrous CH_2Cl_2 solution was injected into the reactor to start polymerization.

Ethylene pressure was maintained at 1 atm (absolute) throughout the polymerization by a continuous feed from the supply cylinder through a bubbler. After a prescribed reaction time (typically, 24 h), the reactor was vented and the polymerization was quenched with acidified methanol (2% HCl), yielding a black oily polymer product. To remove the decomposed Pd catalyst residues, the polymer was dissolved in THF (*ca.* 5 mL), followed by the addition of hydrogen peroxide (1 mL) and hydrochloric acid (1 mL) to digest Pd black. The mixture was then stirred until Pd black completely disappeared. Then the polymer was precipitated in a large volume of methanol, and dried in a vacuum oven at 60 °C for 24 h.

Polymer characterization and analysis

Proton (^1H NMR), carbon-13 (^{13}C) nuclear magnetic resonance, ^1H–^1H correlation spectroscopy (^1H–^1H COSY) and carbon-13 distortionless enhancement by polarization transfer-135 (DEPT-135) spectra of the polymers were obtained on a Bruker 300 MHz spectrometer at ambient temperature. Fluorine-19 nuclear magnetic resonance (^{19}F NMR) spectroscopy, heteronuclear single quantum coherence (^1H–^{13}C HSQC) and hetero-

nuclear multiple bond correlation (^1H–^{13}C HMBC) spectra of the copolymers were obtained on a Varian 500 MHz spectrometer at ambient temperature. Deuterated chloroform was used as the solvent for all the samples for NMR measurements. Differential scanning calorimetry (DSC) analysis was performed on a TA Instruments Q250 DSC under a N_2 atmosphere. The instrument was operated in the standard DSC mode. A N_2 purging flow of 50 mL min^{-1} was used. Samples (about 20 mg) were heated from room temperature to 180 °C at 10 °C min^{-1} and cooled to −90 °C at 5 °C min^{-1}, and then heated again to 180 °C at 10 °C min^{-1}. Data were collected in the cooling step and the second heating step. Glass transition temperature (T_g) was read as the middle of the change in the heat capacity and the melting temperature (T_m) was read as the maximum point of the endotherm peak in the second heating step. Thermogravimetric analysis (TGA) was performed on a TA Instruments Q50 thermogravimetric analyzer. Measurements were carried out under N_2 with a continuous gas flow of 50 mL min^{-1}. A N_2 flow of 40 mL min^{-1} was used as the balance purging gas. In a typical run, the sample was heated from room temperature to 600 °C at a heating rate of 10 °C min^{-1}. Polymer molecular weights, including number-average (M_n) and weight-average (M_w) values, were determined by size exclusion chromatography (SEC) using a Waters 515 high-performance liquid chromatographic (HPLC) pump coupled with a Waters 410 differential refractometer detector and a Waters 996 photodiode array detector operating at a wavelength of 260 nm. A set of Microstyragel columns (100, 500 and 1000 Å) were used for the low-molecular-weight analysis, and another set of Microstyragel columns (103, 104 and 105 Å) were used for the high-molecular-weight analysis. The instrument was calibrated using polystyrene standards with HPLC-grade THF as the mobile phase. Fourier transform infrared (FTIR) spectra were obtained on a Thermo Scientific Nicolet 6700 Analytical FTIR spectrometer.

Results and discussion

Four fluorinated monomers, including HFIPA, APFB, 13FOAE, and PFH, were employed in this work for the synthesis of fluorinated HBPEs by ethylene copolymerization. The monomers, HFIPA, APFB, and 13FOAE, differ in the spacer structure between the vinyl and the fluorinated groups, whereas PFH that has no spacer between the two is included for comparison. While fluorinated acrylates have been reported for copolymerization, APFB, 13FOAE, and PFH have not been previously demonstrated for ethylene copolymerization with Pd–diimine catalysts. APFB and 13FOAE are strategically chosen herein because their distinct spacer structures are expected to reduce catalyst chain walking toward the fluorinated structures during polymerization, thereby promoting successful incorporation.

A classical Pd–diimine catalyst (Pd-1), [(ArN=C(Me)–(Me)C=NAr)Pd(CH$_3$)(N≡CMe)]SbF$_6$ (Ar = 2,6-(iPr)$_2$C$_6$H$_3$), is employed herein for the copolymerization. All the polymerizations were conducted at a low ethylene pressure of 1 atm and

Table 1 Summary of polymerization results and polymer characterization data[a]

Run	Comonomer	[M] (mol L^{-1})	Yield (g)	Act.[b]	TON$_E$[c] (h^{-1})	TON$_{com}$[d] (h^{-1})	Comonomer content[e] (mol%)	M_n[f] (kg mol^{-1})	PDI	Branching[g]/1000C	T_g/T_m[h] (°C)	ΔH_m[h] (J g^{-1})
1	None	N/A	4.57	1.90	68.0	N/A	N/A	26.6	1.53	101	−69.6/−38.2	7.1
2	HFIPA	0.5	3.05	1.27	45.3	0.13	0.3	14.3	1.42	99	−68.5/−34.1	10.9
3	HFIPA	1.0	2.71	1.13	40.1	0.16	0.4	10.9	1.40	98	−68.8/−35.6	9.7
4	APFB	0.5	5.75	2.40	62.5	0.95	1.2	17.4	1.39	95	−66.7/−33.8	7.8
5	APFB	1.0	5.30	2.21	59.8	1.27	1.8	11.9	1.12	93	−65.9/−33.1	6.1
6	13FOAE	0.5	1.91	0.80	21.9	0.45	2.0	2.6	1.47	99	−68.6/−38.7	7.5
7	13FOAE	1.0	1.20	0.50	9.8	0.56	5.4	1.5	1.53	94	−67.8/−39.0	3.9
8	PFH	0.5	5.08	2.12	75.5	—	—	11.9	1.45	98	−68.7/−34.2	11.5
9	PFH	1.0	5.18	2.16	76.9	—	—	12.2	1.39	100	−68.9/−34.7	10.8

[a] Conditions: 0.1 mmol of Pd-1; solvent, CH$_2$Cl$_2$; total volume of polymerization solution, 5 mL; temperature, 25 °C; ethylene, 1 atm; polymerization time, 24 h. [b] Activity (Act.) in kg (mol Pd h)$^{-1}$. [c] TON$_E$ is the ethylene turnover number per hour. [d] TON$_{com}$ is the comonomer turnover number per hour. [e] Comonomer molar percentage in the copolymers determined by ^{1}H NMR spectroscopy. [f] Number-average molecular weight (M_n) and polydispersity index (PDI) determined by SEC. [g] Branching density determined by ^{1}H NMR spectroscopy. [h] Thermal transition temperatures and melting endotherm (ΔH_m) determined by DSC.

a temperature of 25 °C, conditions under which the hyperbranched polymer topology should be obtained following the chain walking characteristics of the catalyst, as demonstrated in our earlier studies.[19–21] For comparison, a hyperbranched polyethylene homopolymer was also synthesized under the same conditions. Table 1 summarizes the polymerization runs and their corresponding conditions. The copolymerizations were performed at two different comonomer feed concentrations (0.5 and 1.0 M, respectively, with the corresponding comonomer to catalyst molar ratios of 25 and 50) to investigate the effects of comonomer concentration on the polymerization behavior and polymer structure.

HFIPA is a semi-fluorinated acrylate, and its analogues with varying fluorocarbon chain lengths have been studied in copolymerization with ethylene using Pd–diimine catalysts. The catalysts are well known to incorporate acrylates at the branch ends with the mechanism well elucidated by Brookhart et al.[19,24]

During polymerization, the ester functionality between the vinyl and the fluorinated alkyl groups effectively blocks catalyst chain walking toward the fluorinated segment after the enchainment of the vinyl group. Meanwhile, the ester group partially shields the electronic effect of the fluorocarbon segment on the reactivity of the vinyl group.

Fig. 1b shows the ^{1}H NMR spectrum of the copolymer produced in run 3 with HFIPA at 1.0 M, and Fig. 1c presents that of the HFIPA monomer for comparison. In the spectrum of the copolymer, characteristic resonances (a′ and b′) resulting from the incorporated HFIPA comonomer can be clearly identified alongside the typical resonances of the branched polyethylene sequences. The resonance peak of the –CH–(CF$_3$)$_2$ group (a′) is centered at 5.77 ppm, shifted slightly upfield compared to that of the comonomer (5.84 ppm, a in Fig. 1c). In addition, a new triplet resonance (b′) centered at 2.51 ppm is found in the copolymer, which is absent in the comonomer, and is attributed to methylene protons next to the carbonyl group (CH$_2$–CH_2–CO(O)) following comonomer incorporation at branch ends. Such a triplet signal at *ca.* 2.3 ppm is typical in ethylene/

acrylate copolymers synthesized using Pd–diimine catalysts, which have the characteristic acrylate enchainment at branch ends.[19,22] The slight shift in its peak position is likely due to the effect of the fluorinated carbon sequence. The presence of these two distinctive signals confirms the successful incorporation of HFIPA in the polymer at branch ends, and its content can be easily quantified from the ^{1}H NMR spectrum.

With HFIPA, relatively low comonomer contents of 0.3 and 0.4 mol% are obtained at feed concentrations of 0.5 and 1.0 M, respectively. This is accompanied by a significant decrease in the catalytic activity from 1.90 in run 1 to 1.27 and 1.13 kg (mol Pd h)$^{-1}$ in runs 2 and 3, respectively, upon comonomer incorporation. Consistently, the turnover number (TON$_{com}$) for HFIPA comonomer incorporation increases from 0.13 to 0.16 h^{-1} with increasing comonomer feed concentration. In contrast, semi-fluorinated acrylates of different fluorocarbon lengths (3 to 17 carbons) were incorporated at 1.25–2.67 mol% with an analogous Pd–diimine catalyst at 1.0–2.0 M feed concentration under 2 atm ethylene and 30 °C, with only minor variation in comonomer content across monomers of different fluorocarbon chain lengths.[17] In contrast, HFIPA in this work exhibits markedly lower incorporation under similar conditions with the classical Pd–diimine catalyst Pd-1, which is attributed to its relatively lower comonomer incorporation efficiency.

In APFB, the vinyl group is separated from the fluorinated carbons of the fluorobenzene ring by an allyl-substituted sp^2 carbon. In previous studies, monomers with a vinyl group directly connected to nonfluorinated benzene, such as styrene, were found to deactivate Pd–diimine catalysts. This occurs because, after the vinyl group is incorporated, the Pd metal center walks to the benzene ring, forming a stable π-benzyl intermediate that inhibits the polymerization.[23] We have previously employed this chemistry to synthesize narrowly distributed ω-telechelic hyperbranched polyethylenes end-capped with reactive functional end groups using functionalized styrene derivatives, including 4-vinylbenzyl chloride, 4-methyl
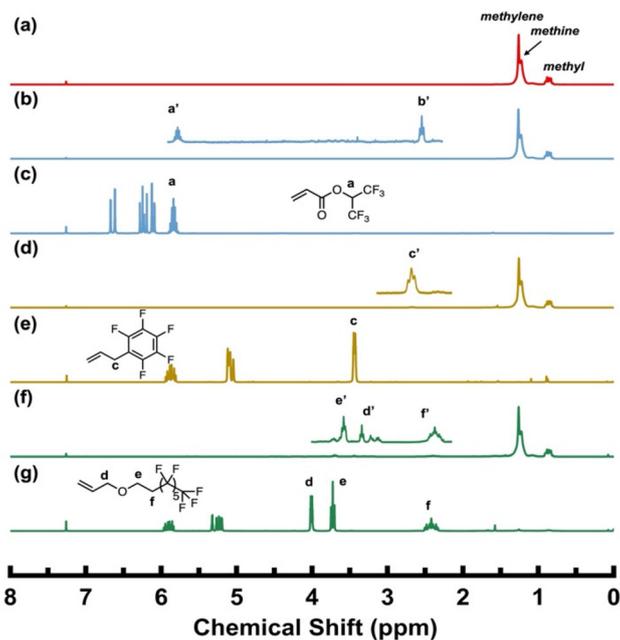
Fig. 1 ^{1}H NMR spectra of (a) homopolyethylene synthesized in run 1, (b) the copolymer of ethylene and HFIPA synthesized in run 3, (c) the HFIPA monomer, (d) the copolymer of ethylene and APFB synthesized in run 5, (e) the APFB monomer, (f) the copolymer of ethylene and 13FOAE in run 7, and (g) the 13FOAE monomer.
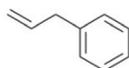
styrene, and divinylbenzene, as end-capping agents.[24] To mitigate the deactivation, we have also examined in this study two monomers bearing an alkyl spacer between the benzene ring and the double bond, allylbenzene and 4-phenyl-1-butene (Scheme 2a), each at a feed concentration of 0.5 M, for copolymerization with ethylene. However, both monomers led to complete deactivation of the Pd–diimine catalyst with no polymer produced, suggesting that merely increasing the spacer length is insufficient to prevent π-benzyl formation. Additionally, ortho-substituted polar allylbenzene monomers containing methoxy (–OMe) and dimethylamino (–NMe₂) groups (Scheme 2b) were previously reported to be ineffective at preventing catalyst chain walking to the benzene ring,

leading to the formation of stable π-benzyl chelates and the subsequent catalyst deactivation.[25] Herein, in APFB, the absence of hydrogen atoms on the pentafluorobenzene structure is expected to effectively prevent catalyst chain walking to the aromatic structure as β-H elimination, a key mechanistic step in chain walking, cannot take place.
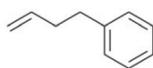
With APFB, successful polymerization was achieved in runs 4 and 5, with catalytic activity even slightly higher relative to the homopolymerization in run 1. Fig. 1d shows the ^{1}H NMR spectrum of the copolymer produced in run 5 (APFB feed concentration: 1.0 M), and Fig. 1e shows the spectrum of the APFB comonomer for comparison. The incorporation of APFB is confirmed by the presence of a characteristic methylene resonance (c′) next to the pentafluorobenzene ring at 2.68 ppm in the copolymer (Fig. 1d), which exhibits a notable upfield shift relative to the corresponding resonance in the comonomer (c at 3.45 ppm). The content of APFB in the copolymers is determined from the ^{1}H NMR spectra and it increases from 1.2 to 1.8 mol% as the comonomer feed concentration increases from run 4 to 5. The comonomer contents in copolymers with APFB are significantly higher than those of the corresponding HFIPA copolymers under otherwise identical polymerization conditions. Meanwhile, catalytic activities with APFB are also appreciably higher than those of the corresponding runs with HFIPA, along with higher TON_{com} of 0.95–1.27 h^{-1} and higher TON_E of 59.8–62.5 h^{-1}. These results indicate that APFB is more efficiently copolymerized than HFIPA with less suppression of catalytic activity in this polymerization system.

The resulting polymers were further characterized with ^{13}C NMR spectroscopy to elucidate their chain microstructures
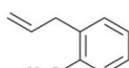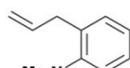

Scheme 2 Alkenyl benzene monomers and ortho-substituted polar allylbenzene monomers leading to the deactivation of Pd–diimine catalysts.
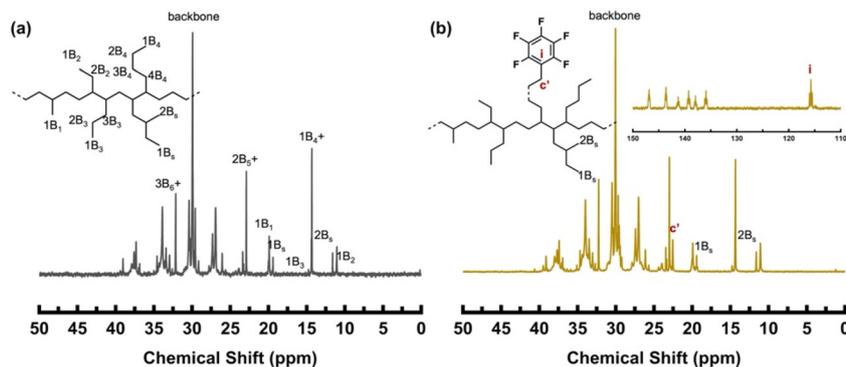
Fig. 2 Representative quantitative ^{13}C NMR spectra of (a) homopolyethylene (run 1) and (b) the copolymer of ethylene and APFB (run 5).

and confirm comonomer incorporation. The ^{13}C NMR spectrum of homopolyethylene produced in run 1 (Fig. 2a) indicates a highly branched structure consisting of methyl, ethyl, *n*-propyl, *n*-butyl, and longer (>4C) side chains, and the shortest branch-on-branch structure, *sec*-butyl branches, (1Bs, 2Bs).[23,26] The ^{13}C NMR spectrum (Fig. 2b) of the ethylene/APFB copolymer (run 5) retains all characteristic resonance peaks seen with homopolyethylene (Fig. 2a). Additionally, new resonances corresponding to carbons c′ and i are clearly identified, along with five distinct fluorinated carbon signals in the region of 135–150 ppm. Relative to other peaks from the ethylene sequence, these additional resonances confirm the successful incorporation of the APFB comonomer into the polyethylene structure.

Subsequently, an allyl fluoroalkyl ether monomer, 13FOAE, was designed and investigated for ethylene copolymerization with Pd-1. In 13FOAE, the long fluoroalkyl is separated from the allyl group with an ether functionality. Previously, α-olefins bearing a terminal ether group have been shown to deactivate Pd–diimine catalysts by catalyst chain walking to the β-carbon next to the ether group followed by β-OR′ elimination. Thus, ether-functionalized α-olefins, even with a long spacer (*e.g.*, eight CH$_2$ units) between the vinyl and ether groups, cannot be copolymerized with ethylene with Pd–diimine catalysts, unless a quaternary carbon that can block catalyst chain walking is designed into the spacer.[15]

Uniquely, ethylene copolymerization with 13FOAE was found to be successful herein. Fig. 1f shows the ^1H NMR spectrum of the copolymer produced in run 7, while Fig. 1g presents the spectrum of the 13FOAE comonomer. Three methylene resonances (d′, e′ and f′) can be clearly identified in the copolymer, corresponding to the respective signals d, e, and f in the comonomer spectrum (Fig. 1g). All three resonances exhibit slight upfield shifts relative to those in the comonomer, with the absence of signals corresponding to the vinyl protons. These results solidly demonstrate that the allyl fluoroalkyl ether comonomer can be successfully copolymerized with ethylene using the Pd–diimine catalyst. Clearly, β-OR′ elimination does not occur in this case with R′ being a long fluoroalkyl group. Notably, at a feed concentration of 1.0 M, the incorporation of 13FOAE reaches 5.4 mol%, indicating the

highest comonomer incorporation efficiency among the three comonomers studied (HFIPA, APFB, and 13FOAE). However, the activity decreases significantly to 0.5 kg (mol Pd h)$^{-1}$ (run 7), significantly lower than 1.9 kg (mol Pd h)$^{-1}$ observed for the homopolymerization (run 1) and the activities achieved in copolymerizations with the other comonomers at the same feed concentration. This reduction in activity may be attributed to the coordination ability of the ether oxygen to the Pd center, which competes with vinyl groups for coordination sites, thereby reducing the ethylene insertion rate.

In the polymerization runs (runs 8 and 9) undertaken in the presence of PFH, the products were found to be ethylene homopolymers with no incorporation of PFH. This is supported by spectroscopic evidence: ^{13}C NMR and FTIR analyses of the polymers obtained in runs 8 and 9 show no resonance peak or vibrational band attributable to incorporated PFH (Fig. 3). These results suggest that PFH cannot be copolymerized with ethylene using Pd-1, even at a feed concentration of 1.0 M. Notably, the presence of PFH does not inhibit ethylene homopolymerization, as the catalytic activity in both runs are comparable to that observed in run 1. This indicates that the vinyl group in PFH cannot bind with the cationic Pd active center for insertion, likely due to the high steric hindrance from the fluoroalkane side group.

Typical of hyperbranched polyethylenes produced with Pd-1, all polymers produced in this study exhibit high branching densities of around 93–100 branches per 1000 carbons, as determined from their ^1H NMR spectra (see Table 1). This high degree of branching is a result of the unique chain walking mechanism of the catalyst. For copolymers produced from each comonomer, increasing the comonomer content leads to a slight decrease in the branching density. This shows that comonomer incorporation slightly reduces the branching density within the ethylene sequences, which is commonly found in ethylene copolymers synthesized using Pd-1, as reported in our earlier works.[22,27–29] It should be noted that differences in chain topology among these copolymers cannot be differentiated by ^1H NMR, as this technique primarily identifies the number of methyl groups at the branch ends and cannot detect branch-on-branch structures.[22,27,30,31]
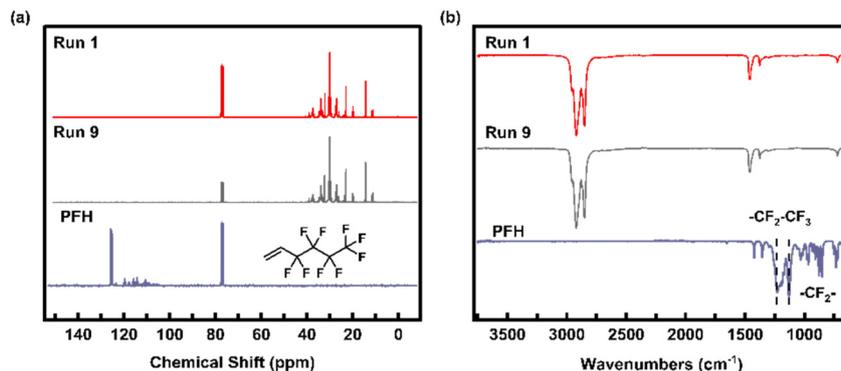
Fig. 3 (a) ^{13}C NMR spectrum and (b) FTIR spectrum of the polymer produced in run 9 in the presence of PFH.

The successful incorporation of fluorinated comonomers has been further confirmed by ^{19}F NMR spectroscopy. As shown in the SI, characteristic fluorine resonances corresponding to each incorporated comonomer are clearly observed in the copolymers, supporting the presence of fluorinated groups in the hyperbranched polyethylenes.

Additional NMR characterization studies have also been performed on representative copolymers to further elucidate the comonomer incorporation pattern in each case. All spectra are provided in the SI. The ^{1}H–^{1}H COSY spectrum of the HFIPA–ethylene copolymer (run 3, Fig. S5) is dominated by extensive correlations arising from the highly branched polyethylene backbone. Notably, no resolvable cross-peaks linking the HFIPA-derived methylene protons (b′) with adjacent polyethylene backbone methylene protons can be identified. Since continuous in-chain incorporation would be expected to generate such diagnostic COSY correlations, their absence argues against main-chain insertion of HFIPA.[32] Similar COSY features are also observed for the APFB–ethylene and 13FOAE–ethylene copolymers (Fig. S13 and S22), indicating an identical incorporation behavior.

For the HFIPA–ethylene copolymer from run 3, DEPT-135 analysis confirmed the HFIPA derived methylene carbon b′ at δC = 33.35 ppm (Fig. S6). Consistently, in the HSQC spectrum, the b′ protons at δH = 2.52 ppm correlate to the methylene carbon signal at δ = 33.35 ppm through $^1J_{CH}$ (Fig. S7), confirming the covalent incorporation of HFIPA at branch ends.[25] Notably, this HSQC cross peak appears as a localized and well-resolved signal, clearly separated from the intense polyethylene backbone methylene correlations (δH = 1.2–1.4 ppm, δC = 29–33 ppm). Importantly, HMBC verifies the long-range correlations of b′ protons with two carbon signals at δC = 24.62 and 170.38 ppm through $^2J_{CH}$ with the methylene carbon m′ and through $^2J_{CH}$ with the carbonyl carbon, respectively (Fig. S8), further confirming the branch-end incorporation of the comonomer.

For the APFB–ethylene copolymer from run 5, a methylene carbon at δC = 29.32 ppm is observed in its DEPT-135 spectrum, corresponding to APFB-derived methylene group n′ (Fig. S14). HSQC (Fig. S15) shows a clear correlation between

the APFB-derived methylene c′ protons (δH = 2.69 ppm) and the corresponding c′ carbon signal at δC = 22.42 ppm through $^1J_{CH}$. Furthermore, HMBC (Fig. S16) reveals long range correlations of c′ protons with two carbons at δC = 29.07 (n′) and 115.31 ppm (i seen in Fig. 2b), respectively, through $^2J_{CH}$. For the 13FOAE–ethylene copolymer from run 7, DEPT-135 (Fig. S23) verifies o′ as a methylene carbon (δC = 29.42 ppm). The methylene d′ proton (δH = 3.45 ppm) correlates to the d′ carbon at δC = 71.44 ppm through $^1J_{CH}$ by HSQC (Fig. S24), to the o′ carbon at δC = 29.42 ppm through $^2J_{CH}$, and to the e′ carbon at 62.63 ppm through $^3J_{CH}$ by HMBC (Fig. S25).

These NMR results solidly demonstrate the exclusive incorporation of the fluorinated comonomers at branch ends, rather than in the main chain. These also prove the formation of copolymers with ethylene, rather than the homopolymers of each fluorinated monomer. The incorporation of the comonomers at branch ends is expected to have minimal impact on the overall chain topology. DSC characterization was carried out to study the thermal properties of the polymers and assess the effects of the incorporation of fluorine-containing monomers. All copolymers are completely amorphous at room temperature due to their hyperbranched structure. Fig. 4 compares the DSC thermograms of the polymers produced in runs 1–7. As reported in our earlier work,[22] the homopolymer in run 1
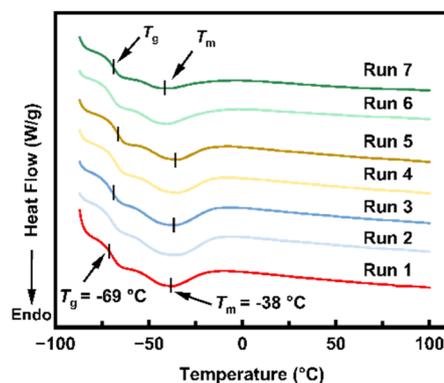

Fig. 4 DSC thermograms of the polymers.

shows a glass transition (T_g) at −69.6 °C, and a weak melting endotherm (ΔH_m = 7.1 J g^{-1}) with a peak maximum (T_m) at −38.2 °C. The copolymers display similar thermal transitions to homopolyethylene, with no new transitions introduced. For a copolymer with a low comonomer content, the impact on thermal properties is minimal. However, for those with higher comonomer incorporation, a slight but notable increase in T_g is observed, along with slight decreases in T_m and ΔH_m (see Table 1). For example, the 13FOAE copolymer produced in run 7 (comonomer content: 5.4 mol%) has a T_g of −67.8 °C, a T_m of −39.0 °C, and a ΔH_m of 3.9 J g^{-1}, which are noticeably different from those of the homopolymer in run 1. These changes suggest that comonomer incorporation hinders the formation of crystallites. Nevertheless, the presence of a weak melting endotherm in all copolymers indicates that fluorinated HBPEs can still crystallize despite their hyperbranched chain structures.[22,27,28,33,34]

TGA measurements were carried out to evaluate the thermal stability of the hyperbranched polyethylene homopolymer (run 1) and representative fluorinated copolymers (runs 3, 5, and 7). The TGA traces are shown in Fig. S40 in the SI, and the corresponding thermal stability data are summarized in Table S1. All polymers exhibit a single degradation step with no distinct pattern of changes observed upon the incorporation of the fluorinated comonomers, indicating that their thermal stability is dominated by the polyethylene backbone. Notably, the 13FOAE–ethylene copolymer (run 7) exhibits a slightly reduced degradation onset temperature ($T_{5\%}$ = 309.5 °C), but with a similar maximum weight loss temperature (T_{max} = 449.8 °C) as other polymers. The slightly earlier onset of mass loss is attributed to the presence of long fluorinated side chains connected through ether linkages, which may undergo minor thermal scission at a lower temperature. Importantly, the similar T_{max} values (450–463 °C) of all polymers confirm that the primary degradation process remains dominated by the polyethylene backbone. Overall, these TGA results indicate that the incorporation of fluorinated comonomers has only limited impact on the thermal stability of the resulting polymers, with the primary chain architecture and degradation behavior largely preserved.

The molecular weights and molecular weight distributions of the polymers were determined with SEC using a refractive index (RI) detector and THF as the eluent at 35 °C. The results are summarized in Table 1. All polymers exhibit monomodal elution curves (Fig. 5a) with a polydispersity index (PDI) of around 1.4–1.5. With the increase of comonomer content in copolymers, the number-average molecular weight (M_n) generally decreases, likely due to enhanced chain transfer or termination events associated with comonomer incorporation. In particular, the 13FOAE copolymers have the lowest M_n values (*i.e.*, 1.5 and 2.6 kg mol^{-1}), corresponding to their high comonomer contents (5.4 and 2.0 mol%, respectively). The homopolymer produced in runs 8 and 9 in the presence of PFH also shows a reduced M_n value (12.2 kg mol^{-1}) in run 9, compared to homopolyethylene (26.6 kg mol^{-1}) in run 1, despite that PFH is not incorporated. This reduction may be attributed to a
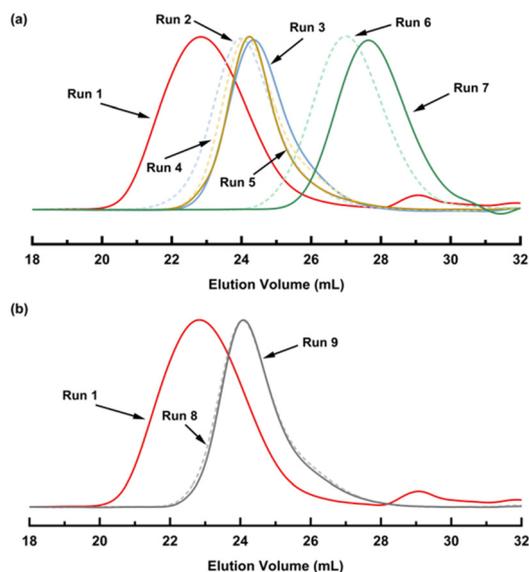

Fig. 5 SEC elution traces (obtained from the DRI detector) of the polymers: (a) runs 1–7; (b) runs 1, 8 and 9.

lower ethylene concentration in the polymerization medium due to the presence of the fluorinated monomer.

Since the fluorinated groups in polymers have a strong tendency to migrate and become enriched at the surface, even small amounts of fluorinated monomer incorporation can significantly influence the surface properties of the resulting polymers.[35] To investigate these effects, water contact angle (WCA) measurements were performed on the polymers. As shown in Fig. 6, the WCA of homopolyethylene produced in run 1 is 90.7°. Incorporation of fluorinated monomers at a feed concentration of 1.0 M leads to a significant increase in WCA: 101.6° for the HFIPA copolymer in run 3, 99.2° for the APFB copolymer in run 5, and 105.4° for the 13FOAE copolymer in run 7. These results clearly demonstrate that the surface hydrophobicity of HBPE has been significantly enhanced by the incorporation of even small amounts of fluorinated monomers. However, the increase in WCA does
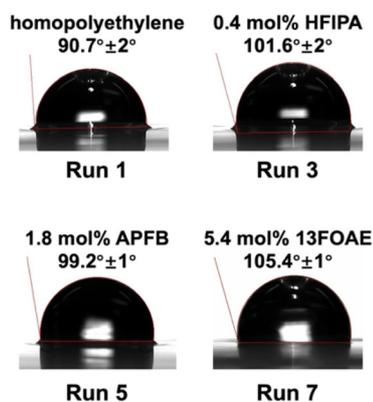

Fig. 6 Water contact angles of homopolyethylene (run 1) and fluorinated copolymers (runs 3, 5, and 7).

not scale linearly with the overall fluorine content across different fluorinated comonomers. This behavior is attributed to differences in fluorinated group structure and chain mobility, which collectively govern surface segregation efficiency.

Conclusions

In summary, fluorinated hyperbranched polyethylenes have been synthesized *via* direct Pd–diimine catalyzed copolymerization of ethylene with three fluorine-containing comonomers having different spacer structures between the vinyl and the fluorinated groups, HFIPA, APFB, and 13FOAE, with the latter two investigated in this study for the first time. The Pd-1 catalyst enables the successful incorporation of all three comonomers, while constructing the hyperbranched polyethylene backbone. Among the comonomers studied, 13FOAE with an ether spacer shows the highest reactivity with Pd-1, followed by APFB with a fluorinated benzene ring, and then the acrylate comonomer HFIPA. At a feed concentration of 1.0 M, 13FOAE achieved the highest comonomer incorporation level of 5.4 mol%, though this was accompanied by a significant reduction in both catalytic activity and polymer molecular weight. In contrast, APFB uniquely maintained the catalytic activity despite achieving a significant comonomer incorporation level of 1.8 mol% at the same feed concentration of 1.0 M. PFH, which has no spacer between the vinyl and the fluorinated alkyl groups, could not be copolymerized using Pd-1, due to the high steric hindrance around the vinyl group. From a structure–reactivity perspective, these results clearly demonstrate that the presence and nature of the spacer between the vinyl functionality and the fluorinated group play a decisive role in monomer reactivity. Incorporation of fluorinated comonomers was found to marginally impact the thermal properties of the polymers. However, significantly enhanced surface hydrophobicity was demonstrated by the incorporation of fluorinated comonomers, even at relatively low contents (up to about 5.4 mol%). Overall, this work provides valuable insights into the rational design of fluorinated comonomers to achieve effective incorporation in hyperbranched polyethylenes using Pd–diimine catalysts.

Author contributions

Peishuai Dai: writing – review & editing, writing – original draft, visualization, validation, resources, methodology, investigation, formal analysis, and data curation. Naiheng Song: resources, formal analysis, and writing – review & editing. Zhibin Ye: conceptualization, writing – review & editing, supervision, resources, project administration, and funding acquisition.

Conflicts of interest

There are no conflicts to declare.

Data availability

The data supporting this article have been included as part of the supplementary information (SI). Supplementary information: NMR spectra, DSC and TGA data, and other relevant experimental results. See DOI: https://doi.org/10.1039/d5py01150g.

Acknowledgements

References

1 H. Peng, *Polym. Rev.*, 2019, **59**, 739–757.
2 B. Ameduri, *Chem. – Eur. J.*, 2018, **24**, 18830–18841.
3 C. Gao and D. Yan, *Prog. Polym. Sci.*, 2004, **29**, 183–275.
4 B. Voit, *J. Polym. Sci., Part A: Polym. Chem.*, 2000, **38**, 2505–2525.
5 J. Wang, Z. Ye and S. Zhu, *Ind. Eng. Chem. Res.*, 2007, **46**, 1174–1178.
6 J. Wang, M. Kontopoulou, Z. Ye, R. Subramanian and S. Zhu, *J. Rheol.*, 2008, **52**, 243–260.
7 L. Xu, Z. Ye, Q. Cui and Z. Gu, *Macromol. Chem. Phys.*, 2009, **210**, 2194–2202.
8 M. Stürzel, S. Mihan and R. Mülhaupt, *Chem. Rev.*, 2016, **116**, 1398–1433.
9 H. Ulrich, *Introduction to industrial polymers*, Hanser, München, New York, 1982.
10 M. M. Marques, S. G. Correia, J. R. Ascenso, A. F. G. Ribeiro, P. T. Gomes, A. R. Dias, P. Foster, M. D. Rausch and J. C. W. Chien, *J. Polym. Sci., Part A: Polym. Chem.*, 1999, **37**, 2457–2469.
11 B. Novak and H. Tanaka, *Abstr. Pap. Am. Chem. Soc.*, 1999, **217**, U414.
12 L. K. Johnson, S. Mecking and M. Brookhart, *J. Am. Chem. Soc.*, 1996, **118**, 267–268.
13 T. R. Younkin, E. F. Connor, J. I. Henderson, S. K. Friedrich, R. H. Grubbs and D. A. Bansleben, *Science*, 2000, **287**, 460–462.
14 F. Wang and C. Chen, *Polym. Chem.*, 2019, **10**, 2354–2369.
15 G. Chen, X. S. Ma and Z. Guan, *J. Am. Chem. Soc.*, 2003, **125**, 6697–6704.
16 S. Mecking, L. K. Johnson, L. Wang and M. Brookhart, *J. Am. Chem. Soc.*, 1998, **120**, 888–899.
17 G. Li, G. Xu, Y. Ge and S. Dai, *Polym. Chem.*, 2020, **11**, 6335–6342.
18 L. W. Devaney and G. W. Panian, *J. Am. Chem. Soc.*, 1953, **75**, 4836–4837.
19 S. Mecking, L. K. Johnson, L. Wang and M. Brookhart, *J. Am. Chem. Soc.*, 1998, **120**, 888–899.

20 Z. Ye and S. Zhu, *Macromolecules*, 2003, **36**, 2194–2197.

21 Z. Ye, F. AlObaidi and S. Zhu, *Macromol. Chem. Phys.*, 2004, **205**, 897–906.

22 J. Wang, Z. Ye and H. Joly, *Macromolecules*, 2007, **40**, 6150–6163.

23 S. D. Ittel, L. K. Johnson and M. Brookhart, *Chem. Rev.*, 2000, **100**, 1169–1204.

24 S. Li and Z. Ye, *Macromol. Chem. Phys.*, 2010, **211**, 1917–1924.

25 X. Hu, X. Ma and Z. Jian, *Polym. Chem.*, 2019, **10**, 1912–1919.

26 P. M. Cotts, Z. Guan, E. McCord and S. McLain, *Macromolecules*, 2000, **33**, 6945–6952.

27 K. Zhang, J. Wang, R. Subramanian, Z. Ye, J. Lu and Q. Yu, *Macromol. Rapid Commun.*, 2007, **28**, 2185–2191.

28 J. Wang, K. Zhang and Z. Ye, *Macromolecules*, 2008, **41**, 2290–2293.

29 S. Morgan, Z. Ye, K. Zhang and R. Subramanian, *Macromol. Chem. Phys.*, 2008, **209**, 2232–2240.

30 Z. Guan, P. M. Cotts, E. F. McCord and S. J. McLain, *Science*, 1999, **283**, 2059–2062.

31 *Metal Catalysts in Olefin Polymerization*, ed. Z. Guan, Springer Berlin Heidelberg, Berlin, Heidelberg, 2009, vol. 26.

32 Y. Zhang, F. Wang, L. Pan, B. Wang and Y. Li, *Macromolecules*, 2020, **53**, 5177–5187.

33 J. Ye, Z. Ye and S. Zhu, *Polymer*, 2008, **49**, 3382–3392.

34 P. Xiang, Z. Ye and R. Subramanian, *Polymer*, 2011, **52**, 5027–5039.

35 A. Otake, M. Miura, K. Tsuchiya and K. Ogino, *J. Photopolym. Sci. Technol.*, 2008, **21**, 679–684.